

Catalysis Science & Technology

Accepted Manuscript



This is an *Accepted Manuscript*, which has been through the Royal Society of Chemistry peer review process and has been accepted for publication.

Accepted Manuscripts are published online shortly after acceptance, before technical editing, formatting and proof reading. Using this free service, authors can make their results available to the community, in citable form, before we publish the edited article. We will replace this *Accepted Manuscript* with the edited and formatted *Advance Article* as soon as it is available.

You can find more information about *Accepted Manuscripts* in the [Information for Authors](#).

Please note that technical editing may introduce minor changes to the text and/or graphics, which may alter content. The journal's standard [Terms & Conditions](#) and the [Ethical guidelines](#) still apply. In no event shall the Royal Society of Chemistry be held responsible for any errors or omissions in this *Accepted Manuscript* or any consequences arising from the use of any information it contains.

Influence of Sulfation and Regeneration on Pt/Al₂O₃ for NO Oxidation

Yuan Li ^a, Meiqing Shen ^{a,b,c}, Jianqiang Wang ^a, Taoming Wan ^a, Jun Wang ^{a,*}

^a Key Laboratory for Green Chemical Technology of State Education Ministry, School of Chemical Engineering & Technology, Tianjin University, Tianjin 300072, PR China

^b Collaborative Innovation Center of Chemical Science and Engineering (Tianjin), Tianjin 300072, PR China

^c State Key Laboratory of Engines, Tianjin University, Tianjin 300072, PR China

* Corresponding author

Tel. +86 22 27892301

E-mail: mqshen@tju.edu.cn

ABSTRACT

Because of the potential crisis that Pt/Al₂O₃ catalysts would be poisoned by S-containing impurities in diesel exhaust, it is expected to better understand the deactivation of SO₂ and regeneration effects on Pt/Al₂O₃ catalysts. In this study, these effects induced by SO₂ over Pt/Al₂O₃ were studied as a function of time of SO₂ exposure, and the NO oxidation activity was performed for different treated Pt/Al₂O₃ catalysts. The results show that the SO₂ exposure period seriously affects the catalytic ability, especially after a long period sulfation process. TEM, CO-DRIFTS, TGA, and STEM-EDS elemental mapping results show that the Pt physical and chemical states, and the SO_x species are considered to be essential parameters in SO_x effects on catalyst. It is found that the partial regeneration in the samples with different SO₂ exposure times is primarily caused by an unrecoverable deactivation of edge and kinked Pt atoms during sulfation process. Moreover, a mechanism of SO_x loading and its elimination through NO oxidation process investigated by *in-situ* DRIFTS provides a further cognizance on the SO_x species and their removal. The mechanism reveals a

special intermediate SO_x species, and thus a possible way that gas SO₂ and O₂ transform to sulfate on catalysts is expected.

KEYWORDS: Diesel oxidation catalysts, Sulfation, Regeneration, NO oxidation, Intermediate species

1. Introduction

Nowadays, environmental problems associated with air pollution are deteriorating our entire earth. These problems represent some of the most formidable challenges facing global society in the future.¹ Some of the leading contributors for air pollution are the pollutants emitted from increasing automobiles. In order to control and degrade these pollutants, a diesel oxidation catalysis (DOC) is considered to be one of the most effective catalysts for diesel engines, which can oxidize CO, HCs, NO and soluble organics to CO₂, H₂O and NO₂. Currently, it has been mostly applied by combining with a diesel particulate filter (DPF) and either a NO_x storage catalyst or a selective catalytic reduction (SCR) catalyst.²⁻⁵ Although the S content in diesel fuel has been drastically reduced through a remarkable de-sulfur technology in the recent years, the sulfur is still one of the most significant factors affecting the performance of various catalysts.^{6,7}

In general, the deactivation mechanism of sulfation are generally divided into three major categories, namely, metal oxide sulfation, support sulfation, and SO_x interactions with water and ammonia in the exhaust.⁸⁻¹⁰ In the metal oxide sulfation studies, Pt is considered to be highly active for SO₂ oxidation, and platinum sulfate formation is not favored.^{11,12} Presence of sulfur oxides in the diesel engine exhaust can be detrimental to the Al₂O₃ support, which ultimately deteriorates the DOC activity.¹³ Even though the sulfation on Al₂O₃ is reversible, this decomposition requires a very high temperature, which results in sintering of the Pt particles and thus decreasing dispersion of Pt on support.¹⁴ Moreover, the sintering of Pt particles leads to an irreversible inactivation, and even reducing lifespan of catalysts.¹⁵⁻¹⁷ Therefore, it is essential that a new and high-efficiency desulfation process needs to be studied and

developed, which would be a guideline to design or improve the DOC catalysts.

In the recent studies, NO oxidation exhibits an outstanding ability to remove SOx. NO_x gas mixtures existed in the diesel exhaust can be applied to regenerate sulfated catalysts, which could replace the traditional thermal regeneration. It was reported by Pazmiño *et al*¹³ that the catalytic activity in SO₂ exposure process was decreased by the formation of Pt-S bond and the Pt-S bond was broken down via NO oxidation to form a Pt-O bond, leading to the regeneration of catalytic activities. However, the influence of SOx near Pt was not considered in the study. On the other hand, although the SOx poisoning located at the different positions around Pt particles were investigated^{7, 18}, the SOx at different locations which may have different influences on Pt particles were ignored.

It is unclear if there is a correlation of distinct location of SOx vs. regeneration effect. Moreover, the SO₂ deactivation and regeneration mechanism of Pt/Al₂O₃ were seldom studied. In the present paper, the impact of SO₂ exposure time on the NO oxidation performance of Pt/Al₂O₃ catalyst samples was systematically investigated and characterized in a standard NO oxidation reaction required by the activated Pt/Al₂O₃ catalysts. SOx species, and their effects on NO oxidation reaction, combining with different SO₂ exposure times, were analyzed, characterized and discussed.

2. EXPERIMENTAL

2.1. Catalyst treatment

Fresh Pt/Al₂O₃ catalyst samples had a ratio of 1.54% SiO₂ addition and a loading fraction of 1.21% Pt. For NO activity tests, powder samples were used, which were loaded in a quartz tube reactor placed inside a temperature-controlled furnace. Before sulfation and regeneration tests, the catalysts were pretreated (activation) by NO oxidation reaction. SO₂ exposure and regeneration processes after the active NO oxidation reaction were alternately carried out. A simulated exhaust gas contained 500

ppm NO, 100 ppm CO, 100 ppm C₃H₆, 5 % CO₂, 3 % H₂O, 10 % O₂ with a balance of N₂ was applied for the NO oxidation reaction of activation and regeneration. The corresponding gas hourly space velocity (GHSV) was 30,000 h⁻¹. The concentrations of influent and effluent gas were controlled by a mass flow meter, and measured by MKS 2030. The reactor was heated from 100 °C to 500 °C at a heating rate of 10 °C/min., and then cooled down to 100 °C in purged N₂. Such a cycle was repeated for another two times. For SO₂ exposure process, the reaction gas mixture consisted of 20 ppm SO₂ with 10 % steam air. The catalysts were treated in the gas mixture atmosphere at 300 °C for 5 hours and 20 hours, respectively. During the treatment processes, the GHSV was constantly controlled by changing the total gas flow. It was noticed that the amount of samples was obviously decreased in the sulfated processes (pick out by FT-IR spectrometer, TGA, and NO activity evaluation test.).

After activation, the catalyst samples were alternatively sulfated for 5 or 20 hours and then regenerated four times. The sulfated samples with three alternated sulfation/regeneration steps for 5 or 20 hours were denoted as 5/20hS-1, 5/20hS-2, and 5/20hS-3, respectively. Similarly, the corresponding regenerated samples were designated as 5/20hR-1, 5/20hR-2, and 5/20hR-3. F represented a fresh sample, while “active” means an activated sample. In order to provide a better insight into this study, a flowchart of the catalyst treatment cycles and process steps is shown in Fig.1.

2.2. Activity measurement

The catalysts activity was conducted on the same kind of flow reactor with NO oxidation reaction and SO₂ exposure process. 0.12 g catalysts mixed with 0.88 g quartz sand was sandwiched between two quartz wool plugs. The gas mixture consisted of 500 ppm NO, 100 ppm CO, 100 ppm C₃H₆, 5 % CO₂, 3 % H₂O, 10 % O₂ with a balance of N₂ was heated from 100 °C to 500 °C at a heating rate of 10 °C /min.

The flow rate was 0.5 l/min, and the corresponding GHSV was 30,000 h⁻¹. The outlet gas was analyzed by MKS 2030. The NO conversion was calculated by the following equation:

$$NO\ Conversion = \frac{[NO]_{inlet} - [NO]_{outlet}}{[NO]_{inlet}} \times 100\%$$

2.3. Catalyst characterization

Transmission electron microscopy (TEM) images were taken using a FEI Tecnai G2 F20 microscope with a field-emission gun operating at 200 kV. STEM-EDS elemental mapping were recorded using a high angle annular dark field (HAADF) detector in the scanning TEM (STEM) energy dispersive X-ray spectroscopy (EDS) mode. The results indicated that the enrichment of Pt generally showed light color, while Al₂O₃-SiO₂ showed the dark color.

Infrared spectra of CO adsorption on the catalysts were recorded on a Nicolet 6700 FT-IR spectrometer equipped with a MCT detector. The catalysts were subjected to a pretreatment at 300 °C with N₂ (300 ml/min) for 30 min, and cooled down to room temperature. At this CO adsorbed temperature, the flow was changed to 1 % CO/N₂ (20 ml/min) for 30 min, and then switched to N₂ (300 ml/min) in order to purge out any residual CO gas existing in chamber.

Thermal gravimetric experiments were conducted on METTLER TOLEDO thermal gravimetric analysis (TGA). 10 mg samples were heated in a mixture gas flow contained N₂ (25 ml/min) and O₂ (5 ml/min) at a heating rate of 10 °C/min from ambient temperature to 1100 °C.

In-situ DRIFTS of SO₂ exposure, desulfation in NO oxidation reaction and investigation of surface SO_x alteration were performed on a NICOLET 6700 FT-IR equipped with a commercial reaction chamber (Thermofisher) at a resolution of 1 cm⁻¹. Ten scans were operated for each spectrum. The subtraction was done at room temperature when the sample background got stable with N₂ purge. Then the catalyst powder samples were heated up from room temperature to 100 °C in N₂ atmosphere. After three cycle's NO oxidation, the pretreatment was completed. SO₂ exposure was measured by introducing freshly mixed 20 ppm SO₂, 20 % O₂, and 2 % H₂O with a balance of N₂ to the chamber at 300 °C. After the SO₂ exposure for 20 hours, the

sample was cooled down to 100 °C, then purged by N₂ to eliminate any residual SO₂ in tubes. In the regeneration process (desulfation in NO oxidation reaction), the sulfated sample was purged in the gas mixture of 500 ppm NO, 100 ppm CO, 100 ppm C₃H₆, 5 % CO₂, 2 % H₂O, 10 % O₂ with a balance of N₂ and heated from 100 °C to 500 °C at a ramping rate of 10 °C/min.

Besides, the surface changes of sulfated sample were respectively investigated by the *ex-situ* DRIFTS in N₂ purged condition and NO oxidation condition (500 ppm NO, 100 ppm CO, 100 ppm C₃H₆, 5 % CO₂, 2 % H₂O, 10 % O₂ with a balance of N₂) with temperature rise from 100 °C to 500 °C at a ramping rate at 10 °C/min. Differed with a fresh sample as a reference spectrum in the *in-situ* DRIFTS experiment, a sulfated sample was used as reference spectrum so as to clearly investigate the changes in the *ex-situ* DRIFTS experiment.

3. RESULTS AND DISCUSSION

3.1. SO₂ exposure impact on NO oxidation activity

NO oxidation performance of 5h-S catalyst as a function of temperature is shown in Fig. 2a. An approximate 70 % NO conversion is obtained in the first cycle at 300 °C. After two more NO oxidation cycles, the NO conversion further increases to more than 80 % in the temperature range of 220 to 300 °C, which almost reaches the activity level of active catalyst, indicating that the activity of the sample is recovered.

NO oxidation performance of 20hS catalyst as a function of temperature is shown in Fig. 2b. A long time exposure of catalyst to SO₂ leads to a lower NO conversion (less than 60 % at 330 °C). After the 2nd and 3rd cycles, the 20hR catalyst is only partially regenerated. An approximate 75 % NO conversion at 300 °C is achieved, compared to 80 % one of the 5hR catalyst in a wider temperature of 200-300 °C. In the rest of 5 and 20 hours sulfated catalysts, the resemblance is described in Fig.S1 and 2.

The effect of reaction temperature on NO oxidation performances of catalyst

samples with different sulfated times, regeneration cycles and circular steps for sulfation/regeneration, are shown in Fig. 3. The NO conversion of the 5 hour sulfated sample for the first cycle has only 70 % at 300 °C (Fig. 3a). However, after two cycles regeneration, the NO oxidation activity is almost completely recovered, and NO conversion values are reached to the same with that of the active catalyst sample (Fig.3c). These results indicate that the cycle time in regeneration plays an important role in the activation of NO oxidation reaction.

As shown in Fig. 3b and d, the 20 hour sulfated sample exhibits a similar behavior as the 5 hours one. However, it should be noticed that, even though the sample is regenerated for three cycles, the activation of NO oxidation is only partially recovered, leading to lower NO conversions. It is obvious that the activation of the catalysts is seriously deteriorated with increasing SO₂ exposure time, and cannot be completely regenerated by NO oxidation.

The sulfation time also affects on the NO_x storage. It is seen from Fig. S3 that the long time SO₂ exposure sample has less NO_x storage than that of the short time sulfated sample. However, the NO_x storage is not considered as a major factor which significantly influences on the NO conversion. A major reason is that the NO conversion strongly depends on the Pt active sites. An obvious decrease of Pt active site caused by increasing SO₂ exposure time will lead to a serious decline of NO conversion. Further, the less NO₂ generation on the long time SO₂ exposed catalyst leads to less NO_x storage on support. Besides, the storage amount of NO_x on Pt/Al₂O₃ catalyst is generally very minor. Therefore, the influence of NO_x storage on Pt/Al₂O₃ catalyst is ignorable compared with that of Pt activity on the catalyst.^{19, 20}

3.2.Morphology and size of Pt by HRTEM

Generally, NO oxidation over Pt catalysts is believed to depend strongly on the particle size of Pt^{21, 22}. Pt particles are investigated by high-resolution TEM, and shown in Fig.4. Compared the Pt particle size of a fresh sample with those of sulfated and regenerated samples, it is found that the Pt particles show almost no

changes on the morphology and size after a long time SO₂ exposure treatment or through a process of NO oxidation, indicating that the deactivation of SO₂ exposure has little relation with Pt particle size. In other word, the low NO conversion after SO₂ exposure and unrecoverable deactivation are possibly caused by the chemical variation instead of the size of Pt particles.

3.3.SO_x location and distribution by STEM-EDS elemental mapping

The images of SO_x distribution on both Pt and support obtained by STEM-EDS mapping are shown in Fig. 5. HAADF images can show an entire view at the interested part of catalyst samples. It is determined that the lighter and well distributed dots are Pt particles, while the darker areas are the support. The distribution mappings of element Pt and S in scanning square region 1 are shown in two small inserted images, respectively. It is seen from Fig. 5a that S element has a high concentration at the same location with Pt particles, indicating that SO_x prefers to accumulate on Pt rather than on the support. After the sulfated catalyst sample is regenerated, the concentration of SO_x around Pt is obviously dispersed (see Fig. 5b), which indirectly indicates that the decomposition of SO_x on Pt is easier than that located on the support during regeneration process.

Combined the result of the stability of Pt particle size during the various treatments with the inactive property of the support on NO oxidation reaction, it is reasonably deduced that the changes of Pt produced by SO_x may result in the unrecoverable deactivation of catalyst.

3.4.State of Pt by CO-DRIFTS method

More specific details of the SO_x species differing from each other are discussed by investigating the adsorption ability of Pt on CO molecule. Fig. 6 shows the DRIFTS spectra of CO adsorption on the catalyst samples at room temperature. The

fresh sample exhibits three overlapped bands at 2092-2024, 2105 and 2130 cm^{-1} which are assigned to CO linearly adsorbed on Pt^0 crystallites, Pt electron-deficient clusters ($\text{Pt}^{\delta+}$) and PtO, respectively.²³⁻²⁶ As the active site of NO oxidation on Pt/ Al_2O_3 catalyst is Pt^0 , the amount of linear CO adsorption on Pt^0 directly reflects the amount changes of active sites. As shown in Fig. 6a, after the catalyst sample is sulfated, the broad band at 2092-2024 cm^{-1} decreases, especially for the long time SO_2 exposure catalyst. That is because the surface of Pt particles, in subsequently sulfated processes, is deposited by different amounts of SO_x , which leads to the changes of these bands. After regeneration process, the regenerated catalyst exhibits a higher IR absorbency around 2092-2024 cm^{-1} than the sulfated catalyst because of the partially removal of SO_x and the re-exposure of Pt, providing more adsorption sites for CO after the regeneration process. More subtle division of the range 2092-2024 cm^{-1} of IR absorbency is attributed to the CO molecules adsorbed at three different positions of Pt atom on Pt particle. The Pt atoms at three positions are the Pt atom belonged to terrace surface of Pt (2092-2083 cm^{-1}), the Pt atom on the edge of Pt particles (2063 cm^{-1}) and the Pt atom at the kinked Pt particles (2024 cm^{-1})^{23, 27}, respectively. The change tendency of different kinds of Pt is classified by dividing the broad peaks, and the results are listed in Table 1 and shown in Fig. 6b. It is worth to mention that the band around 2092 cm^{-1} (CO adsorbs on terrace Pt) slightly shift to a high wavenumber. It is known that the residual SO_x in regeneration samples has a strong capability of absorption electrons and thus captures electrons for Pt. In this case, the non-poisoned Pt in the sulfated and regenerated catalysts remains a thinner electronic cloud than that of active Pt/ Al_2O_3 catalyst, which results in the shifting of CO adsorption.

After 5 hours SO_2 exposure, the CO adsorption on all kinds of Pt is decreased, and then recovered after NO oxidation reaction. However, Pt atoms at three different positions show distinguished abilities in the elimination of SO_x . Although the terrace Pt^0 is almost recovered, the edge and kinked Pt^0 can only partially be regenerated. It is known that SO_2 , as a large electron supplier like CO, prefers to first adsorb on the kinked Pt, and then the edge Pt, and finally the terrace Pt, making SO_x be easier formed on the kinked Pt.²⁸ This preference also makes the generated SO_x always

easily be formed but more difficult be decomposed. A model which illustrates the formation of SO_x on Pt particles is shown in Fig.7.

In addition, it is observed from Fig. 6 that the bridged CO on Pt (1840 cm^{-1})²³ also decreases or even disappears in both 5 and 20 hour catalyst systems, indicating that Pt sites are occupied by SO_x, and as the result, the two adjacent Pt capable of forming CO bridged absorption are reduced. Such a tendency is observed in all of sample systems (in Fig. S4).

3.5. Quantification of SO_x species by TGA

The SO_x decomposition processes of the catalyst samples at elevated temperatures under O₂/N₂ atmosphere were studied by TGA. In general, the weight loss below 200 °C is related to the evaporation of water, and the weight loss over 450 °C is attributed to the decomposition of SO_x.²⁹ Because the stabilities of different kinds of SO_x are distinguished from each other, SO_x species corresponds to a distinct decomposition temperature. It is seen from TG results (see Fig. S5) that the sulfated and subsequently regenerated samples heated in the O₂/N₂ atmosphere show a drastic weight loss above 450 °C. Relatively, the regenerated samples have a less mass loss than the sulfated ones.

Derivative TG curves (DTG) were obtained from the TGA data and shown in Fig.8. Three different decomposition temperatures, which are centered around 570 (A), 750 (B) and 870°C (C), respectively, are explicitly observed, in accordance with those of theoretical analysis.^{26, 29, 30} In the 5 hours sulfated and corresponding regenerated samples (in Fig. 8a), the amount of SO_x loss for both sulfated and regenerated samples is minor at 570 °C, but larger amount of SO_x decomposition is observed around 750 and 870 °C. Differently, much more SO_x are formed on the 20 hours catalysts system during SO₂ exposure process (Fig. 8b), especially at low temperature (570 °C), and more SO_x remains on the regenerated samples as well.

In order to get a quantitative analysis, the amount of SO_x with different

decomposition temperatures were calculated and shown in Fig. 9. In the 5 hours sulfated sample system (Fig. 9a), the SO_x species “A” with a low decomposition temperature of 570 °C is formed slightly during SO_x exposure process and almost decomposed during NO oxidation reaction. In contrast, in the 20 hours sulfated sample system (Fig. 9b), the longer the SO₂ exposure time, the more the SO_x deposited on Pt. However, a drastic change of the SO_x species “A” is observed, i.e. a large amount of the species “A” formed in sulfation process is almost decomposed during NO oxidation process. The SO_x species “B” significantly formed in both 5 and 20 hours sulfation process is partially decomposed during NO oxidation. However, due to a longer time SO₂ exposure, the more “B” are accumulated on the 20 hours sulfated samples, and thus the remains are more than those on the 5 hours sulfated samples as well. The SO_x species is much less sensitive to NO oxidation process. Before and after NO oxidation process, the SO_x species “C” almost keeps constant. That is observed in both 5 and 20 hours sample systems.

Consequently, as the sulfated samples for 5 or 20 hours are regenerated, the SO_x “A” is mostly decomposed, the “B” are partially decomposed, and the “C” keeps constant. It is known from the quantified results of CO-DRIFTS (see Table 2) that the “A” is little generated and mostly recovered (more than 50%), and about one third of the “B” and “C” are done in the 5 hours sulfated sample system after the NO oxidation process. Similarly, the most of “A” is also recovered, but only a small portion of “B” and “C” (20%) is done in the 20 hours sulfated sample system. Combined the SO_x change results detected by TGA with the Pt state results obtained by CO-DRIFTS, it is well reasonable that the SO_x species “A” is classified as the SO_x on the terrace Pt⁰, the “B” as one on the edge and kinked Pt⁰. The “C” is possibly related to the SO_x on the support [Al₂(SO₄)₃]. More specific results about the correlation between the amounts of Pt sites changes and the changes of SO_x are also listed in Table 2. It is seen that the SO_x on terrace is easier to be removed and the SO_x on edge Pt is nest, while the SO_x on kinked Pt is very stable and thus the kinked Pt is hard to be recovered.

Therefore, the NO oxidation ability can be reasonably related with different

types of SO_x on catalysts. Specifically, those SO_x species located at edge and kinked Pt, considerably poison the active capability of Pt and thus results in the deactivation of catalysts. Furthermore, the regeneration of catalysts is primarily controlled by the edge and kinked Pt. In this case, a long time SO₂ exposure on catalysts leads to more SO_x remains located at the edge and kinked Pt after the regeneration process, and thus deteriorated the NO oxidation ability. The possible processes how the SO_x forms during SO₂ exposure and decomposes during NO oxidation are discussed in the next section.

3.6. *In-situ* and *ex-situ* measurement of SO_x location and its removal by DRIFTS

The SO_x species and their differences in the sulfation and NO oxidation regeneration processes were characterized by the means of *in-situ* pool of DRIFTS.

The catalyst samples were exposure in the gas of 20 ppm SO₂, 1.5 % H₂O and 20 % O₂ at 300 °C for 20 hours. The *in-situ* DRIFTS spectra of the samples are shown in Fig.10. With increasing exposure time, the intensity of different bands increases significantly in the band range from 1050 to 1450 cm⁻¹, which are attributed to different SO_x species on catalysts. The sulfate on aluminum is found around 1110 cm⁻¹.^{29, 31-33} The intense bands at 1182 cm⁻¹ and 1257 cm⁻¹ are attributed to S-O vibration in sulfate and SO₃ on Pt, respectively.³⁴⁻³⁷ A gradually saturated peak found at 1358 cm⁻¹ is considered to be the vibration of S=O. As the spectra is shown, when the Pt/Al₂O₃ sample is exposed to SO₂ under oxidizing conditions, the SO_x at 1358 cm⁻¹ is formed quickly, then some other SO_x (at 1110, 1182 and 1257 cm⁻¹) are formed at the beginning of the SO₂ exposure. With further increasing exposure time up to 5 and even more hours (continuously expose to SO₂ and O₂ with H₂O), the intensity of band 1358 cm⁻¹ no longer increases. Even though the band of 1358 cm⁻¹ gets saturated, others bands at 1257 and 1182 cm⁻¹ keep growing with increasing SO₂ exposure times. In addition, the band at 1110 cm⁻¹ grows much slowly after 5 hour exposure because of the limitation of SO_x accumulation on support.³⁸

In the regeneration process shown in Fig. 10b, surprisingly, a broad peak from 1075 to 1450 cm^{-1} , instead of the multi-peaks in Fig. 10a, is observed. With the increase of temperature, the band near 1370 cm^{-1} (1358 cm^{-1} in sulfation process) is observed while the intensity of bands near 1293 cm^{-1} (1257 cm^{-1}) and 1182 cm^{-1} (1193 cm^{-1}) decreased. This special band near 1370 cm^{-1} attributed to the vibration of S=O band^{31,37}, mentioned above, is considered as an unstable SOx species on Pt, which might be an intermediate SOx species during the formation and decomposition of SOx. Consequently, it is rationally assumed that the SOx first prefers to form an intermediate species on Pt. The structure of this intermediate species is schematically shown in Fig. 11, in which exhibits an unstable connection of adsorbed SO₂ and dissociated adsorbed O between two Pt atoms. It seems that the formation of the intermediate SOx is necessary during both sulfation and regeneration processes. It is thought that during SO₂ exposure process, the unstable intermediate SOx first transforms to Pt-SO₃, and then Pt-SO₃ transfers to Pt-SO₄ by gradually oxidation. The regeneration process should be a converse process of the sulfation. In addition, the NO oxidation provides a driving force to make the converse decomposition of SOx occurred during the regeneration process.

In order to identify the effect of gas compositions on sulfated samples, a sulfated sample was heated from 100 °C to 500 °C in N₂ purge and NO oxidation conditions, respectively. The results obtained *ex-situ* DRIFT spectra for the sulfated samples are shown in Fig.12. At the beginning of the temperature programmed experiment, the band corresponding to the intermediate SOx is not observed in both N₂ purge and NO oxidation conditions at the temperatures below 200 °C (Fig. 12a). However, a broad band centered at 1370 cm^{-1} , which is regarded as the intermediate SOx, increases fast after 200 °C. Therefore, the temperature is regarded as an infector which affects or activates if the SOx transforms into the unstable intermediate species on Pt.

In addition, the effect of NO oxidation gas composition on the transformation of the intermediate SOx species is investigated and shown in Fig.12b. Similarly to the band changes with temperatures in Fig.12a, a band at 1376 cm^{-1} increases with increasing temperature. But differently, a negative peak at 1270 cm^{-1} is observed. It is

proved in the N_2 purge experiment that NO gas composition promotes the transformation of SO_x near Pt. Consequently, the SO_x is activated and transformed to intermediate SO_x with temperatures, and then this kind of unstable intermediate SO_x is decomposed during NO oxidation. In addition, the species Pt-SO₃ is easy to be broken down (agreed with the results of TGA and CO-DRIFTS), which makes a negative peak at 1270 cm^{-1} .

4. CONCLUSIONS

The regeneration of the sulfated catalysts by NO oxidation is systematically investigated. The results show that the short-time sulfated catalyst can be almost completely recovered, but the long-time sulfated ones could not be totally regenerated. In addition, the alternant processes between the sulfation and regeneration provide an efficient way to keep the catalyst to be re-activated.

The effect of SO₂ poisoning on NO oxidation activity of a Pt/Al₂O₃ catalyst is characterized. The regenerated extent of catalyst activation is related to the remains of SO_x on the catalysts. The SO_x species located on support of catalysts has a little contribution to the poisoning, but is also hard to be removed by NO oxidation. The SO_x related with the terrace Pt⁰ affects NO oxidation of catalysts and is easy to be removed. The SO_x species located on the kinked and edge Pt⁰ could be partially removed by NO oxidation. These SO_x species are responsible for the unrecoverable deactivation.

A possible process mechanism of regeneration and sulfation is proposed, shown in Fig. 11. During the sulfation process, an intermediate species is formed after the chemical adsorption. Then the intermediate species is oxidized and transformed to SO₃. The SO₃ are further transformed to a more stable sulfate Pt-SO₃ by connecting with Pt. Correspondingly, during the regeneration process, the SO_x species are transformed to the unstable intermediate SO_x species in the NO oxidation condition, and finally are removed. These processes are reversible based on the DRIFTS results.

ACKNOWLEDGMENTS

The authors would like to acknowledge the financially supported provided by the BASF Corporation, and the National Natural Science Foundation of China (Grant No. 21476170)

Supporting Information

The following results are included in Appendix section. NO conversion profiles of other sulfated samples, IR spectra of CO-DRIFTS of other sulfated and corresponding regenerated samples, TG results of all the sulfated and regenerated samples.

REFERENCES

- 1 N. S. Hom, L. S. Steven and B. M. Ashish, in *Novel Materials for Catalysis and Fuels Processing*, American Chemical Society, 2013, vol. 1132, pp. 117-155.
- 2 J. C. Clerc, *Appl. Catal., B*, 1996, **10**, 99-115.
- 3 K. Hauff, U. Tuttlies, G. Eigenberger and U. Nieken, *Appl. Catal., B*, 2012, **123-124**, 107-116.
- 4 R. D. Clayton, M. P. Harold, V. Balakotaiah and C. Z. Wan, *Appl. Catal., B*, 2009, **90**, 662-676.
- 5 M. Iwasaki and H. Shinjoh, *Appl. Catal., A*, 2010, **390**, 71-77.
- 6 X. Wei, X. Liu and M. Deeba, *Appl. Catal., B*, 2005, **58**, 41-49.
- 7 E. C. Corbos, X. Courtois, N. Bion, P. Marecot and D. Duprez, *Appl. Catal., B*, 2008, **80**, 62-71.
- 8 J. A. Rodriguez and J. Hrbek, *Acc. Chem. Res.*, 1999, **32**, 719-728.
- 9 R. Burch, E. Halpin, M. Hayes, K. Ruth and J. A. Sullivan, *Appl. Catal., B*, 1998, **19**, 199-207.
- 10 D. L. Mowery, M. S. Graboski, T. R. Ohno and R. L. McCormick, *Appl. Catal., B*, 1999, **21**, 157-169.
- 11 E. Xue, K. Seshan and J. R. H. Ross, *Appl. Catal., B*, 1996, **11**, 65-79.
- 12 G. Corro, *React. Kinet. Catal. Lett.*, 2002, **75**, 89-106.
- 13 J. H. Pazmiño, J. T. Miller, S. S. Mulla, W. Nicholas Delgass and F. H. Ribeiro, *J. Catal.*, 2011, **282**, 13-24.
- 14 D. H. Kim, Y.-H. Chin, G. G. Muntean, A. Yezeretz, N. W. Currier, W. S. Epling, H.-Y. Chen, H. Hess and C. H. F. Peden, *Industrial & Engineering Chemistry Research*, 2006, **45**, 8815-8821.
- 15 Y. Nagai, T. Hirabayashi, K. Dohmae, N. Takagi, T. Minami, H. Shinjoh and S. i. Matsumoto, *J. Catal.*, 2006, **242**, 103-109.

- 16 A. Borgna, F. Normand, T. Garetto, C. R. Apesteguia and B. Moraweck, *Catal. Lett.*, 1992, **13**, 175-188.
- 17 W. S. Epling, L. E. Campbell, A. Yezerets, N. W. Currier and J. E. Parks, *Catalysis Reviews*, 2004, **46**, 163-245.
- 18 A. Y. Stakheev, P. Gabrielsson, I. Gekas, N. S. Teleguina, G. O. Bragina, N. N. Tolkachev and G. N. Baeva, *Top. Catal.*, 2007, **42-43**, 143-147.
- 19 L. Olsson, H. Persson, E. Fridell, M. Skoglundh and B. Andersson, *The Journal of Physical Chemistry B*, 2001, **105**, 6895-6906.
- 20 Z. Liu and J. A. Anderson, *J. Catal.*, 2004, **224**, 18-27.
- 21 S. Mulla, N. Chen, L. Cumarantunge, G. Blau, D. Zemlyanov, W. Delgass, W. Epling and F. Ribeiro, *J. Catal.*, 2006, **241**, 389-399.
- 22 A. Boubnov, S. Dahl, E. Johnson, A. P. Molina, S. B. Simonsen, F. M. Cano, S. Helveg, L. J. Lemus-Yegres and J.-D. Grunwaldt, *Appl. Catal., B*, 2012, **126**, 315-325.
- 23 J. Raskó, *J. Catal.*, 2003, **217**, 478-486.
- 24 A. Bourane, *J. Catal.*, 2001, **202**, 34-44.
- 25 F. Boccuzzi, A. Chiorino and E. Guglielminotti, *Surf. Sci.*, 1996, **368**, 264-269.
- 26 S. Liu, X. Wu, D. Weng, M. Li and J. Fan, *Appl. Catal., B*, 2013, **138-139**, 199-211.
- 27 B. E. Hayden, K. Kretzschmar, A. M. Bradshaw and R. G. Greenler, *Surf. Sci.*, 1985, **149**, 394-406.
- 28 R. K. Brandt, M. R. Hughes, L. P. Bourget, K. Truszkowska and R. G. Greenler, *Surf. Sci.*, 1993, **286**, 15-25.
- 29 P. T. Fanson, M. R. Horton, W. N. Delgass and J. Lauterbach, *Appl. Catal., B*, 2003, **46**, 393-413.
- 30 B. Li and R. D. Gonzalez, *Appl. Catal., A*, 1997, **165**, 291-300.
- 31 H. Abdulhamid, E. Fridell, J. Dawody and M. Skoglundh, *J. Catal.*, 2006, **241**, 200-210.
- 32 J. M. Jones, V. A. Dupont, R. Brydson, D. J. Fullerton, N. S. Nasri, A. B. Ross and A. V. K. Westwood, *Catal. Today*, 2003, **81**, 589-601.
- 33 L. Li, Q. shen, J. Cheng and Z. Hao, *Catal. Today*, 2010, **158**, 361-369.
- 34 D. Uy, K. A. Wiegand, A. E. O'Neill, M. A. Dearth and W. H. Weber, *The Journal of Physical Chemistry B*, 2001, **106**, 387-394.
- 35 H. Mahzoul, L. Limousy, J. F. Brillhac and P. Gilot, *J. Anal. Appl. Pyrolysis*, 2000, **56**, 179-193.
- 36 Y. Su and M. D. Amiridis, *Catal. Today*, 2004, **96**, 31-41.
- 37 M. Happel, N. Luckas, F. Viñes, M. Sobota, M. Laurin, A. Görling and J. r. Libuda, *The Journal of Physical Chemistry C*, 2010, **115**, 479-491.
- 38 M. Bensitel, M. Waqif, O. Saur and J. C. Lavalley, *The Journal of Physical Chemistry*, 1989, **93**, 6581-6582.

FIGURE CAPTIONS

Figure 1. Flowchart of detailed processes in this study.

Figure 2. (a) NO conversion over 5hS-1 sample for 3 NO oxidation cycles and comparison of

activated sample (b) NO conversion over 20hS-1 sample for 3 NO oxidation cycles and comparison of activated sample. The gas composition includes 500 ppm NO + 100 ppm CO + 100 ppm C₃H₆ + 10 % O₂ + 5 % CO₂ + 3 % H₂O balanced N₂ and the space velocity was 30,000 h⁻¹.

Figure 3. NO conversion comparison between 5 and 20 sulfated samples (a) 5h sulfated samples (1st cycle) (b) 20 h sulfated samples (1st cycle) (c) 5h sulfated samples (3rd cycle) (d) 20h sulfated samples (3rd cycle). The gas composition includes 500 ppm NO + 100 ppm CO + 100 ppm C₃H₆ + 10 % O₂ + 5 % CO₂ + 3 % H₂O balanced N₂ and the space velocity was 30,000 h⁻¹.

Figure 4. TEM images of (a) fresh sample; (b) 5hS; (c) 5hR; (d) 20hS; and (e) 20hR samples.

Figure 5. Full vision catalyst by HAADF detector and STEM-EDS elemental map of S and Pt of the selected region (a) 5hS; (b) 5hR; (c) 20hS; (d) 20hR samples. *Note: Region 2 and spot 1 were selected to contrast the relative changes of sample positions during the STEM elemental map scanning, and captured in the images.

Figure 6. IR spectra of CO adsorption on the different treatment catalysts (a) 5hS, 5hR, 20hS and 20hR; (b) relative amount of different Pt on Pt particles by integral computation and normalization based on the amount of terrace Pt⁰ in active catalyst.

Figure 7. Simple model of Pt particles and the relative position of SO_x related with Pt atom (terrace Pt⁰, edge Pt⁰ and kinked Pt⁰)

Figure 8. Derivative data of weight loss of fresh, activated, sulfated and corresponding regenerated samples during temperature programmed process in 20 % O₂/N₂ atmosphere (a) 5 hours sample system (b) 20 hours sample system.

Figure 9. The amount of SO_x of different species and the variation tendency of SO_x before and after regeneration; (a) 5 hours sample system, (b) 20 hours sample system.

Figure 10. DRIFT spectra for the Pt/Al₂O₃ sample (a) after exposure to 20 ppm SO₂, 1.5 % H₂O and 20 % O₂ in N₂ at 300 °C for 0 – 20 hours; (b) during NO oxidation process (500 ppm NO, 100 ppm CO, 100 ppm C₃H₆, 5 % CO₂, 1.5 % CO₂, 10 % O₂ and balanced N₂) with 10 °C/min heating rate from 30 °C to 500 °C.

Figure 11. The possible assumption of intermediate species model and the assumption of the mechanism of change of SO_x during the sulfation and regeneration processes.

Figure 12. DRIFT spectra for the sulfated sample in (a) N₂ purge and (b) NO oxidation gas composition with a 10 °C/min heating rate.

Table 1. The amount of Pt of different physical and chemical properties at various positions.

	PtO	Pt^{deta+}	terrace Pt⁰	edge Pt⁰	kinked Pt⁰
active	0	0.126	1	0.701	0.577
5hS	0.011	0.162	0.627	0.351	0.253
5hR	0.013	0.113	0.779	0.413	0.255
20hS	0.032	0.022	0.135	0.045	0.016
20hR	0.041	0.077	0.790	0.301	0.102

Table 2. The correlation between deactivate Pt and amount of SO_x on sulfated and regenerated catalysts.

		<i>Active cat.</i>			<i>5 hours cat. system</i>			<i>20 hours cat. system</i>		
		Terrace Pt (T)	Edge Pt (E)	Kinked Pt (K)	Terrace Pt	Edge Pt	Kinked Pt	Terrace Pt	Edge Pt	Kinked Pt
<i>Sulfated</i>	(T+E+K)/all Pt	0.9390			0.5075			0.0805		
	T(E/K)/all Pt	0.4122	0.2888	0.2380	0.2586	0.1445	0.1044	0.0555	0.0184	0.0065
	Deactivate Pt/origin Pt	-	-	-	0.3725	0.4997	0.5616	0.8653	0.9361	0.9726
	Amount of SO _x (mg)	-	-	-	0.0331	0.1108		0.2006	0.1992	
<i>Regenerated</i>	(T+E+K)/all Pt	-			0.5966			0.4916		
	T(E/K)/all Pt	-	-	-	0.3212	0.1701	0.1053	0.3256	0.1242	0.0419
	Deactivate Pt/origin Pt (after regeneration)	-	-	-	0.2207	0.4111	0.5578	0.2102	0.5701	0.8241
	Recovered ratio	-	-	-	40.8%	17.7%	0.7%	75.7%	39.1%	15.3%
	Amount of remain SO _x (mg)	-	-	-	0.0119	0.0721		0.0078	0.1462	
	Decrease of SO _x (mg)	-	-	-	0.0212	0.0387		0.1928	0.0530	
	SO_x Removal ratio	-	-	-	64.0%	34.9%		96.1%	26.6%	

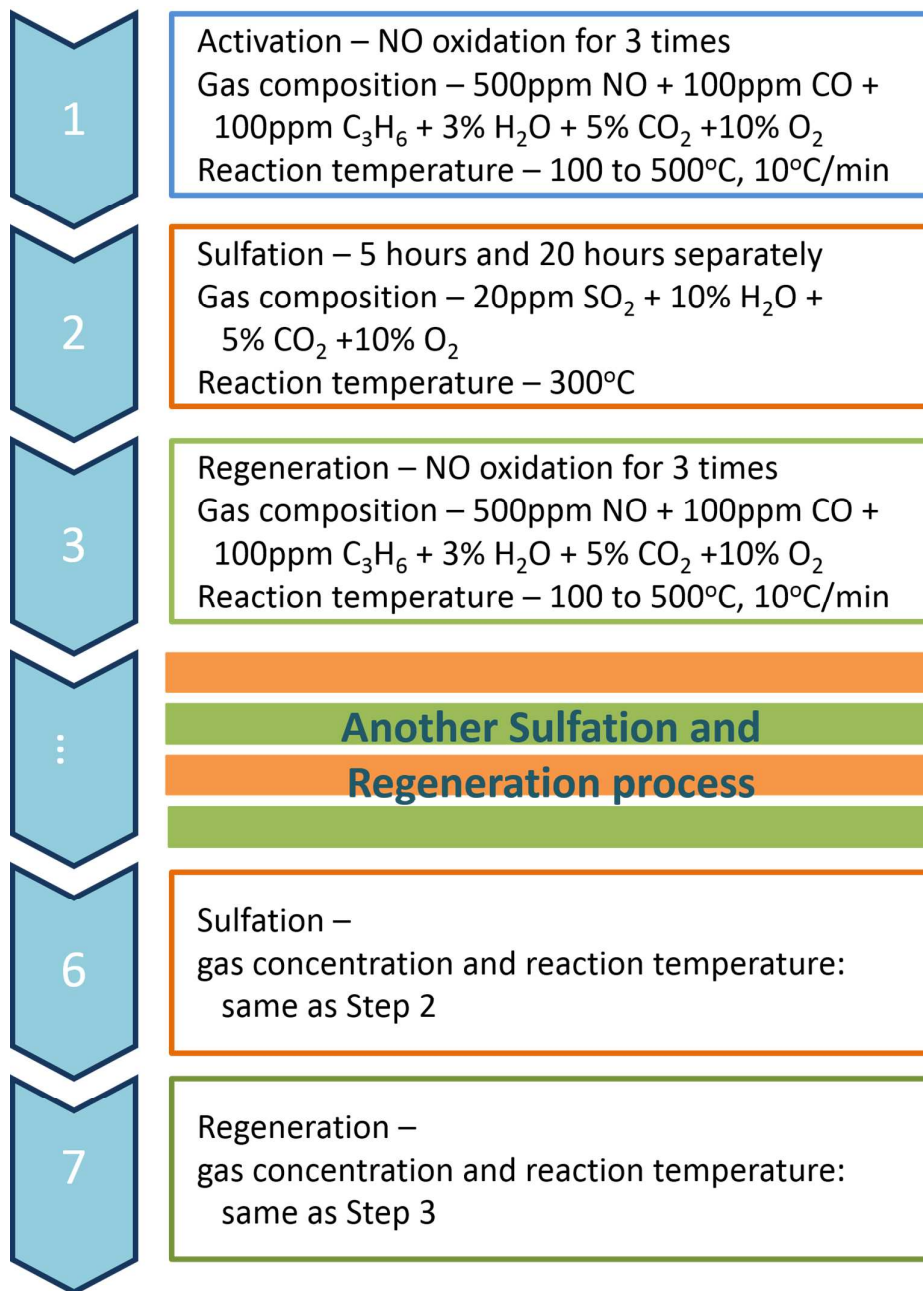


Figure 1. Flowchart of detailed processes in this study.

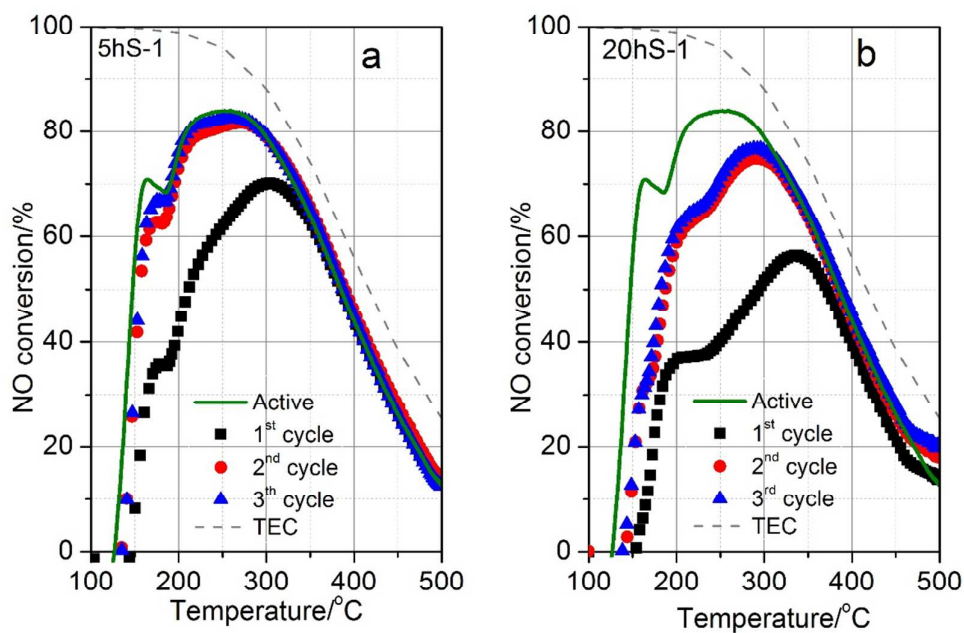


Figure 2. (a) NO conversion over 5hS-1 sample for 3 NO oxidation cycles and comparison of activated sample (b) NO conversion over 20hS-1 sample for 3 NO oxidation cycles and comparison of activated sample. The gas composition includes 500 ppm NO + 100 ppm CO + 100 ppm C₃H₆ + 10 % O₂ + 5 % CO₂ + 3 % H₂O balanced N₂ and the space velocity was 30,000 h⁻¹.

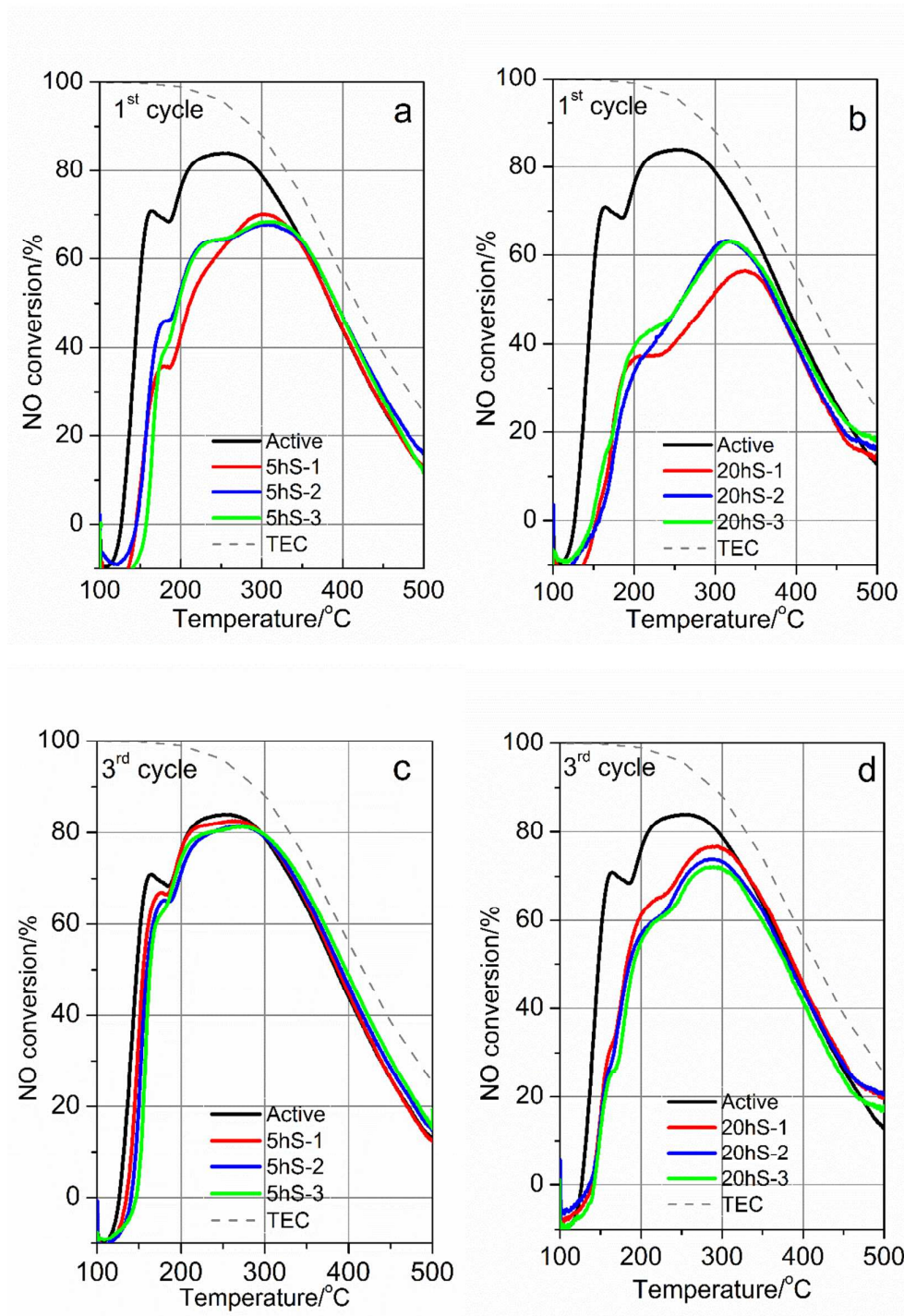


Figure 3. NO conversion comparison between 5 and 20 sulfated samples (a) 5h sulfated samples (1st cycle) (b) 20 h sulfated samples (1st cycle) (c) 5h sulfated samples (3rd cycle) (d) 20h sulfated samples (3rd cycle). The gas composition includes 500 ppm NO + 100 ppm CO + 100 ppm C₃H₆ + 10 % O₂ + 5 % CO₂ + 3 % H₂O balanced N₂ and the space velocity was 30,000 h⁻¹.

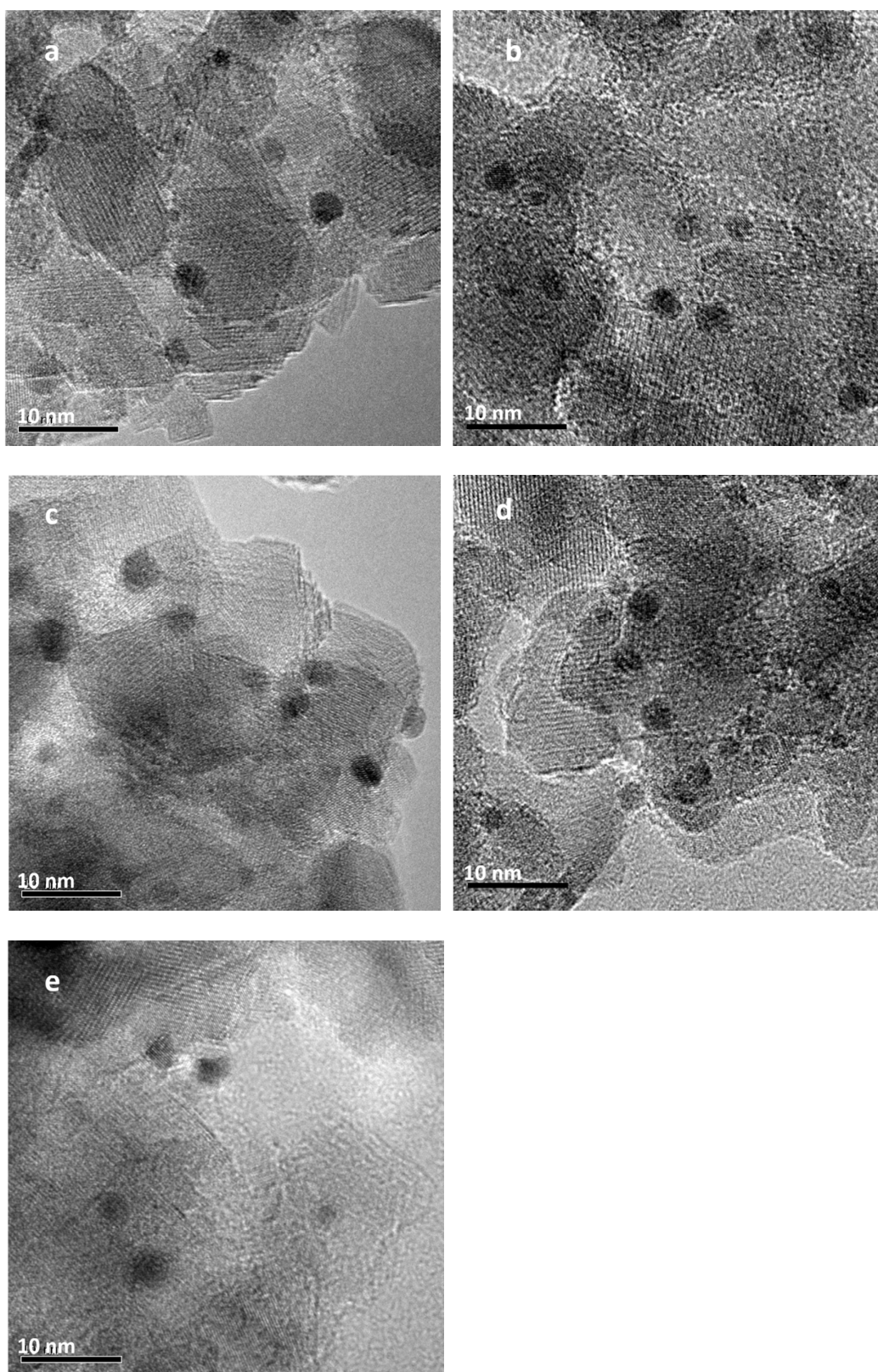
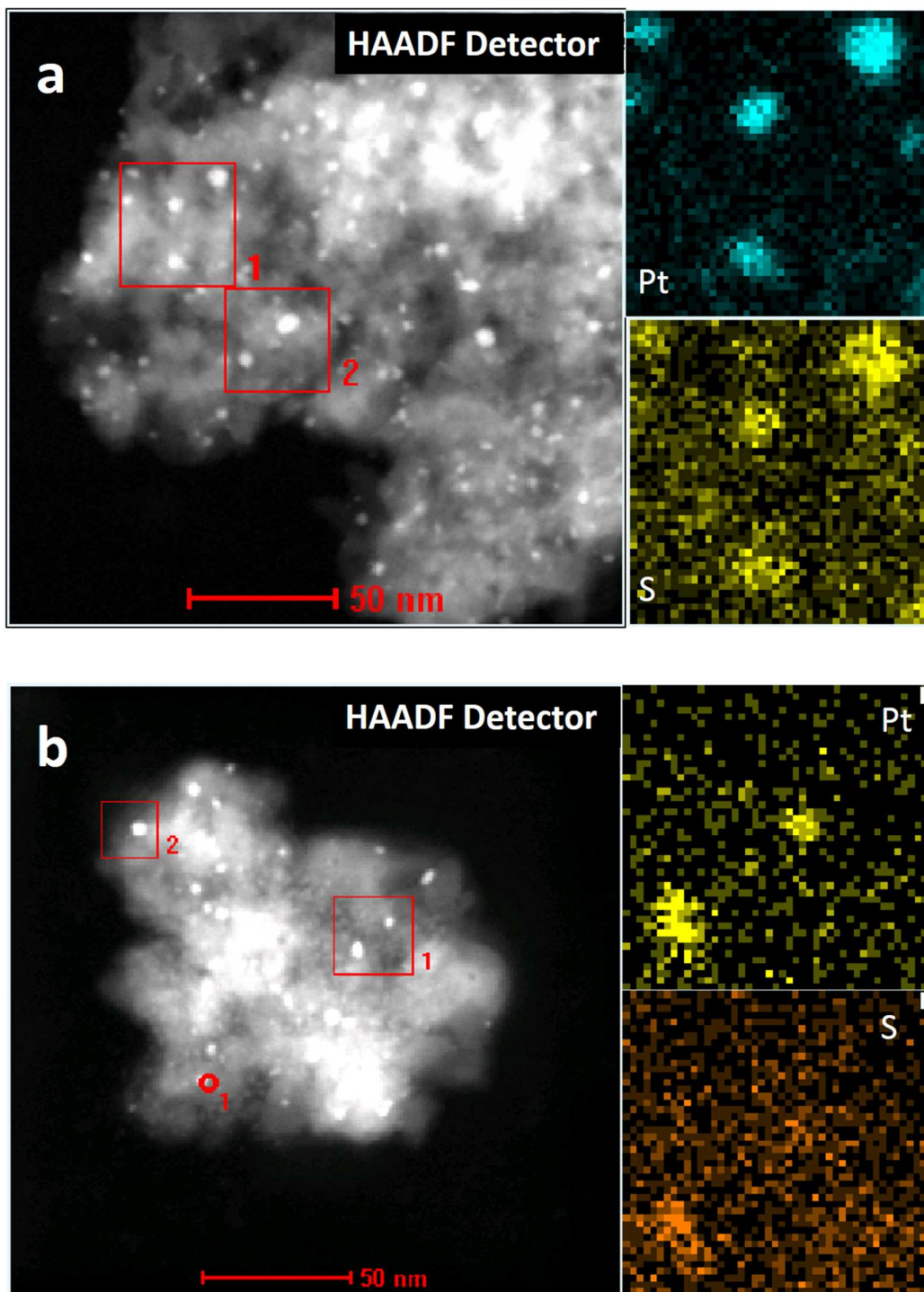


Figure 4. TEM images of (a) fresh sample; (b) 5hS; (c) 5hR; (d) 20hS; and (e) 20hR samples.



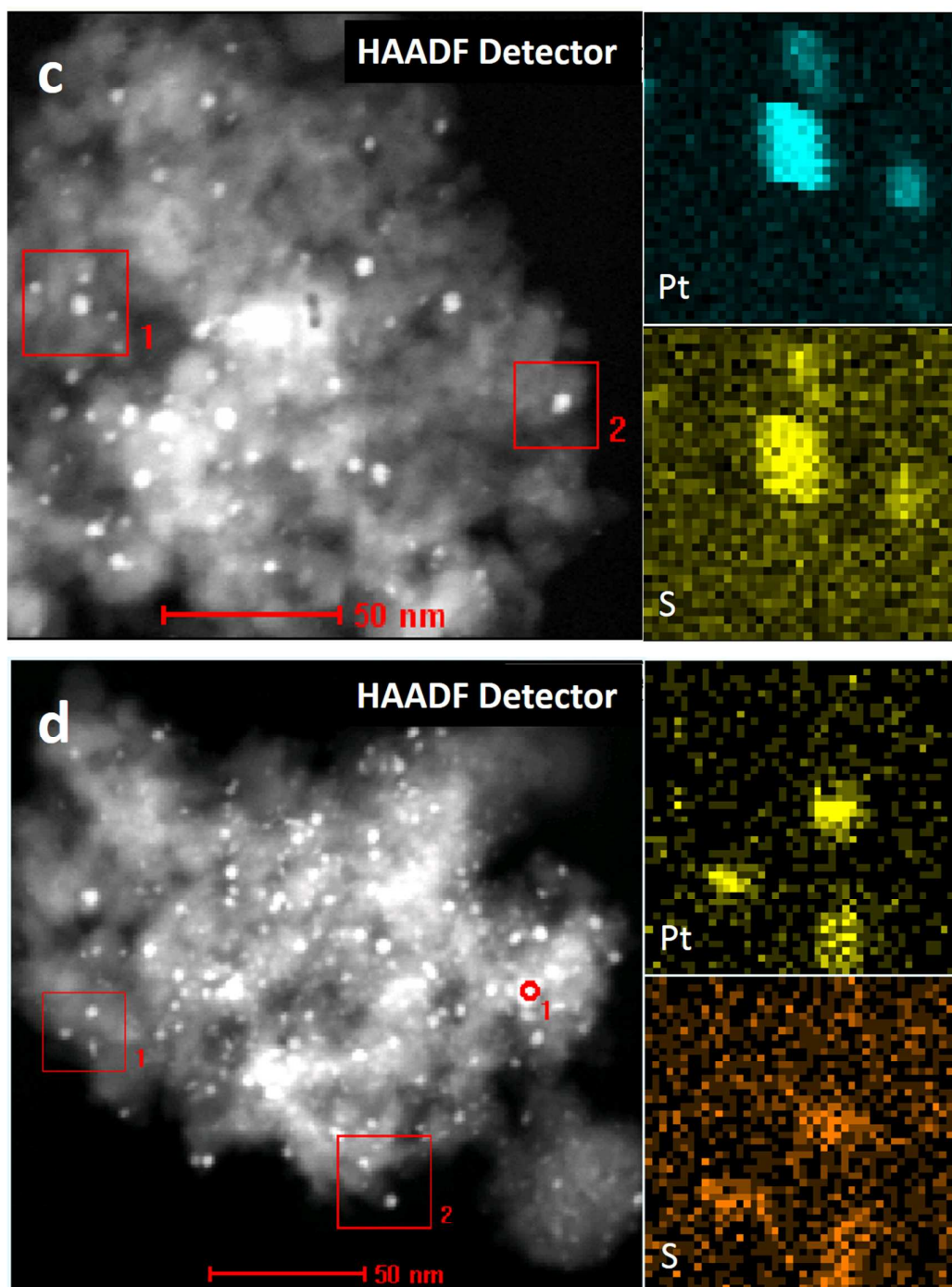


Figure 5. Full vision catalyst by HAADF detector and STEM-EDS elemental map of S and Pt of the selected region (a) 5hS; (b) 5hR; (c) 20hS; (d) 20hR samples. *Note: Region 2 and spot 1 were selected to contrast the relative changes of sample positions during the STEM elemental map scanning, and captured in the images.

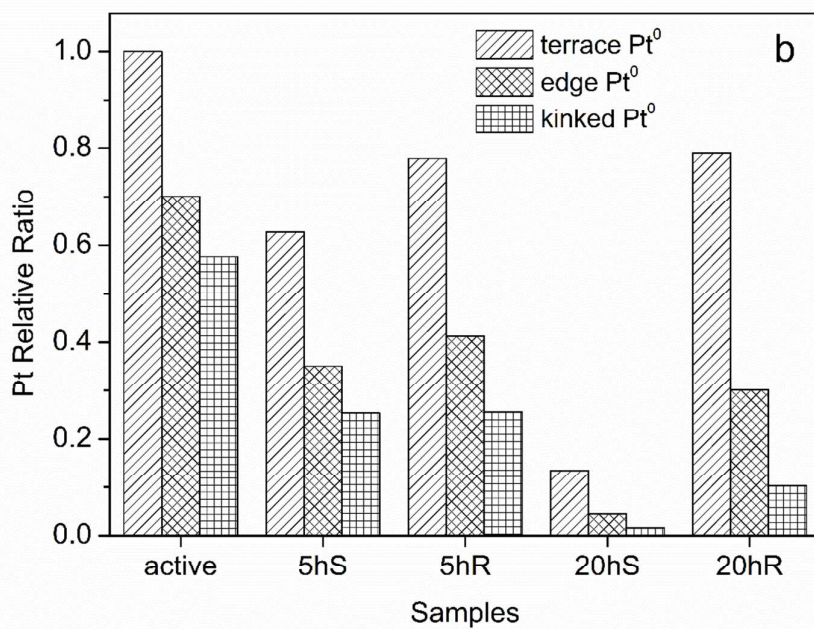
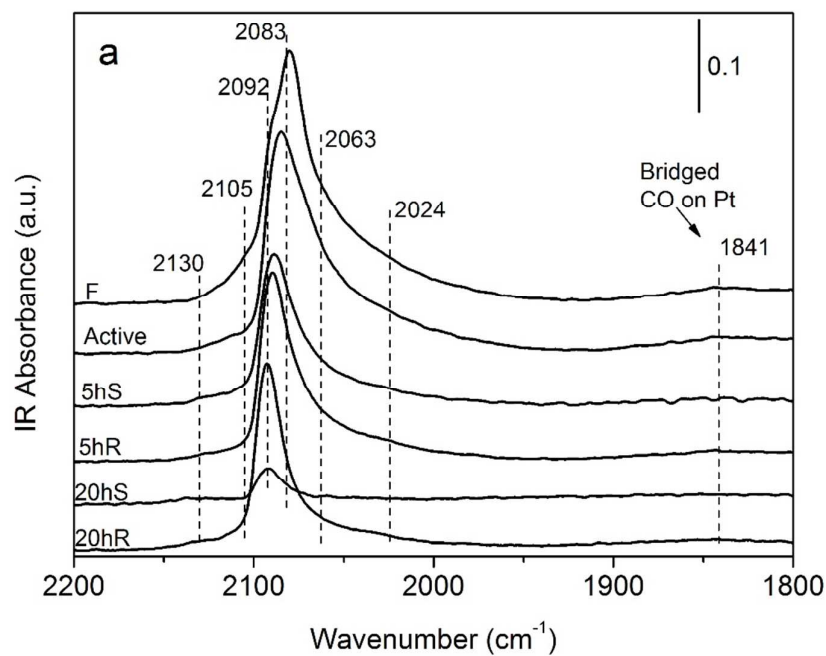


Figure 6. IR spectra of CO adsorption on the different treatment catalysts (a) 5hS, 5hR, 20hS and 20hR; (b) relative amount of different Pt on Pt particles by integral computation and normalization based on the amount of terrace Pt⁰ in active catalyst.

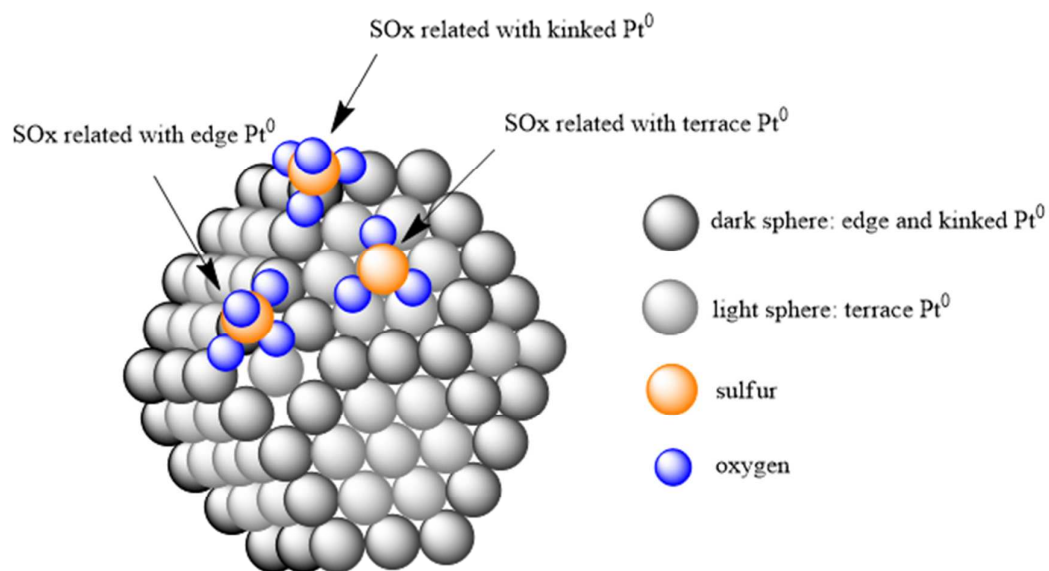


Figure 7. Simple model of Pt particles and the relative position of SOx related with Pt atoms (terrace Pt⁰, edge Pt⁰ and kinked Pt⁰)

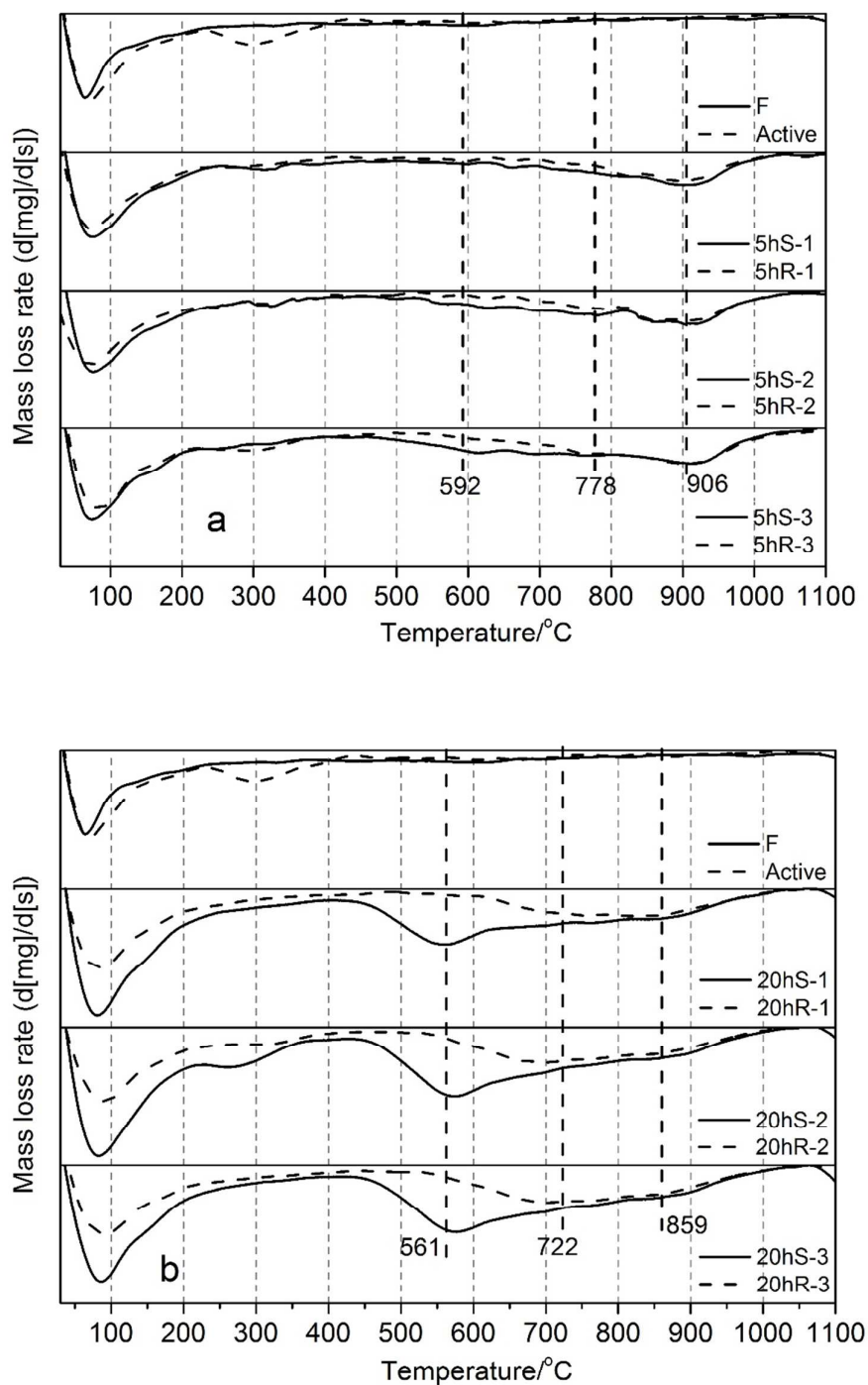


Figure 8. Derivative data of weight loss of fresh, activated, sulfated and corresponding regenerated samples during temperature programmed process in 20 % O₂/N₂ atmosphere (a) 5 hours sample system (b) 20 hours sample system.

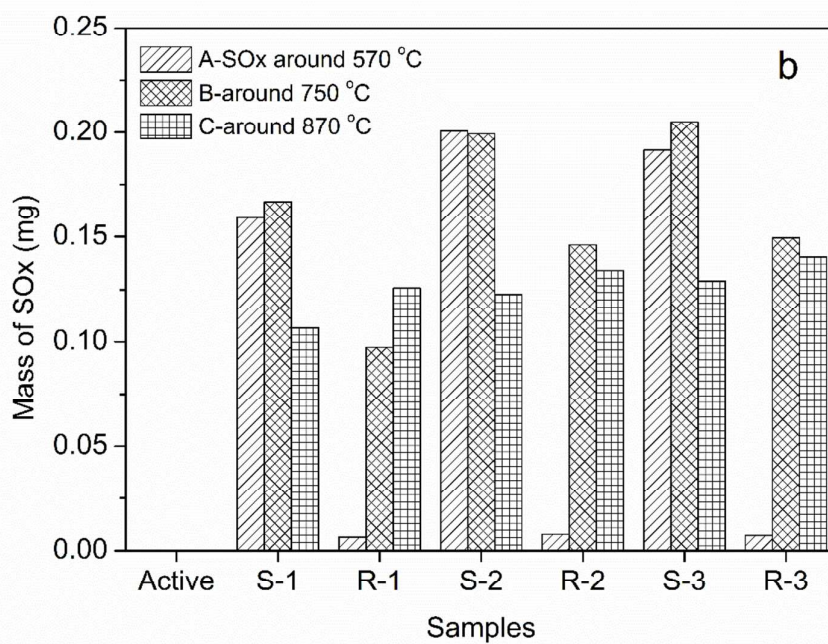
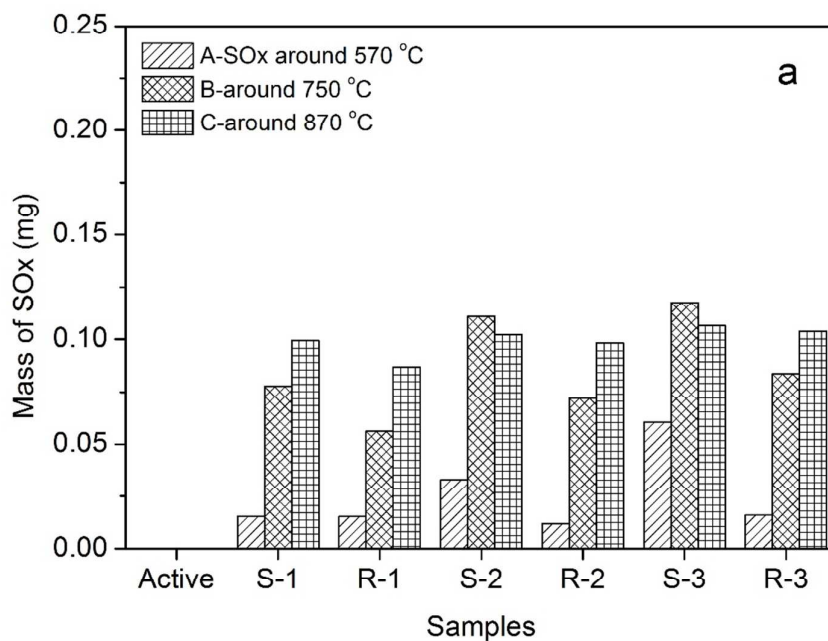


Figure 9. The amount of SOx of different species and the variation tendency of SOx before and after regeneration; (a) 5 hours sample system, (b) 20 hours sample system.

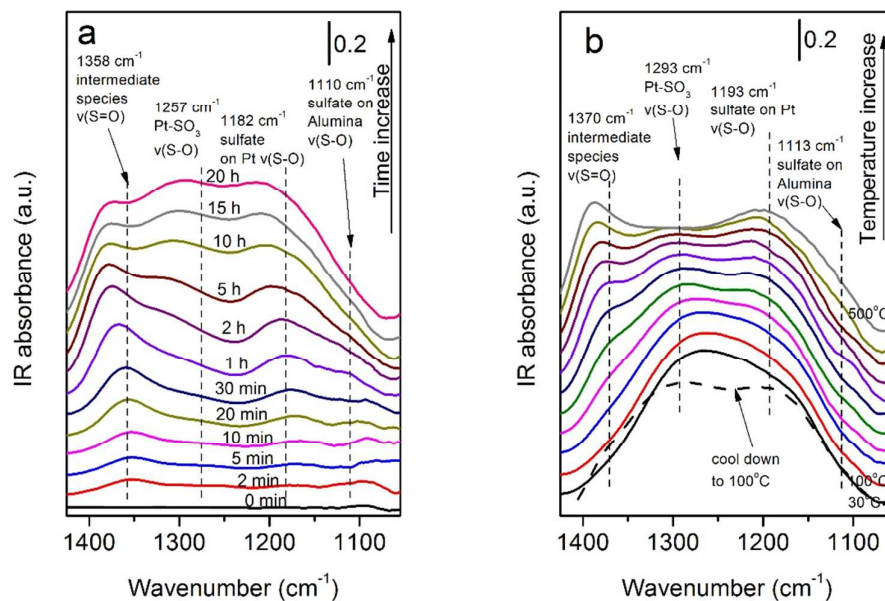


Figure 10. DRIFT spectra for the Pt/Al₂O₃ sample (a) after exposure to 20 ppm SO₂, 1.5 % H₂O and 20 % O₂ in N₂ at 300 °C for 0 – 20 hours; (b) during NO oxidation process (500 ppm NO, 100 ppm CO, 100 ppm C₃H₆, 5 % CO₂, 1.5 % CO₂, 10 % O₂ and balanced N₂) with 10 °C/min heating rate from 30 °C to 500 °C.

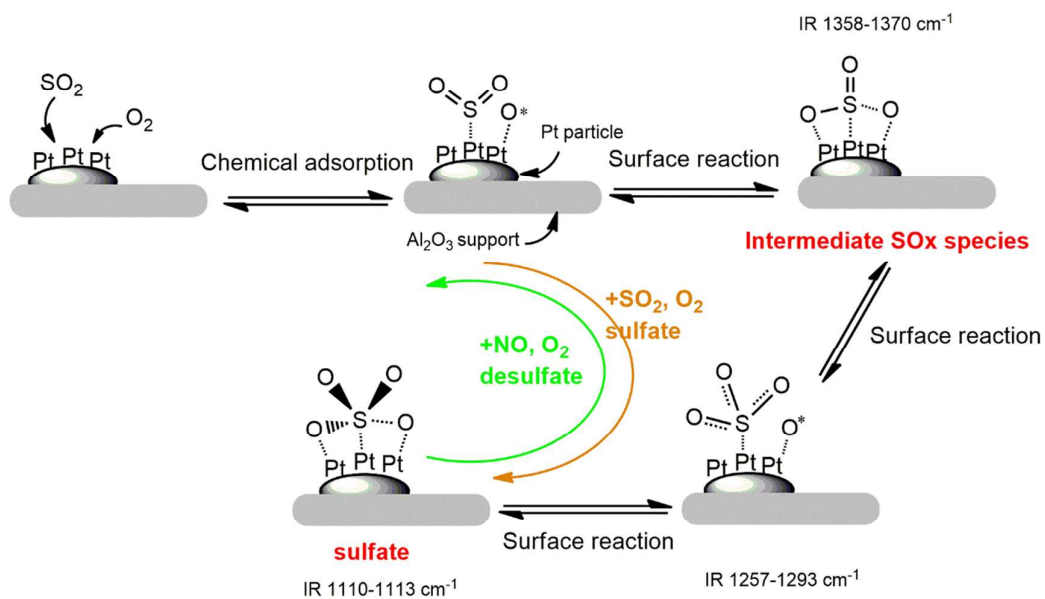


Figure 11. The possible assumption of intermediate species model and the assumption of the mechanism of change of SO_x during the sulfation and regeneration process.

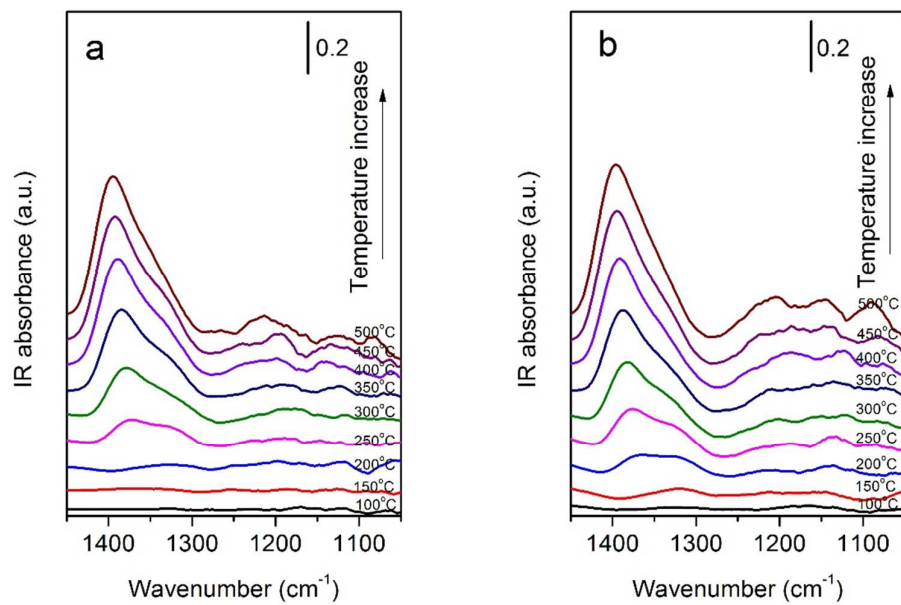


Figure 12. DRIFT spectra for the sulfated sample in (a) N₂ purge and (b) NO oxidation gas composition with a 10 °C/min heating rate.